The American Journal of Pathology, Vol. 170, No. 2, February 2007

DOI: 10.2353/ajpath.2007.060433

Immunopathology and Infectious Disease

Impairment of Functional Capillary Density but Not Oxygen Delivery in the Hamster Window Chamber during Severe Experimental Malaria

Judith Martini,* Irene Gramaglia,† Marcos Intaglietta,*† and Henri C. van der Heyde†

From the Department of Bioengineering, University of California, San Diego; and the La Jolla Bioengineering Institute,† La Jolla, California*

Microcirculatory changes and tissue oxygenation were investigated during *Plasmodium berghei*-induced severe malaria in the hamster window chamber model, which allows chronic, noninvasive investigation of the microvasculature in an awake animal. The main finding was that functional capillary density, a parameter reflecting tissue viability independent of tissue oxygenation, was reduced early during the course of disease and continued to decline to ~20% of baseline of uninfected controls on day 10 after infection. Parasitized red blood cells and leukocytes adhered to arterioles and venules but did not affect overall blood flow, and there was little evidence of complete obstruction of blood flow. According to the sequestration hypothesis, obstruction of blood flow by adherent parasitized erythrocytes is the cause of tissue hypoxia and, eventually, cell death in severe malaria. Tissue oxygen tensions were lower on day 10 of infection when the animals were moribund compared with uninfected controls, but this level was markedly higher than the lethal threshold. No necrotic cells labeled with propidium iodide were detected in moribund animals on day 10 after infection. We therefore conclude that loss of functional capillaries rather than tissue hypoxia is a major lethal event in severe malaria. ***(Am J Pathol 2007, 170:505–517; DOI: 10.2353/ajpath.2007.060433)***

Severe malaria is a clinical syndrome involving many organs and presenting with a variety of clinical symptoms such as coma, seizures, respiratory distress, hypoglycemia, and metabolic acidosis.[1] Metabolic acidosis, in particular lactic acidosis (blood lactate ≥5 mmol/L), is an independent prognostic factor for lethal outcome of severe malaria.[2–4] The most important cause for the development of lactic acidosis is believed to be an increased rate of anaerobic glycolysis of infected tissues, triggered by microvascular obstruction and therefore reduced oxygen delivery to tissues.[5–7] This hypothesis originates from observations of the Italian pathologists Marchiafava and Bignami more than a century ago, who described a phenomenon currently termed "sequestration," namely the trapping of parasitized erythrocytes in the brain microvessels of patients who succumb due to severe malaria. These autopsy results and the observed lactic acidosis are the basis for the sequestration hypothesis, which proposes that adherent parasitized erythrocytes obstruct the vessel lumen, impede blood flow, and impair tissue oxygenation.[1,6] Syrian golden hamsters infected with *Plasmodium berghei* exhibit similar parasitized erythrocyte and leukocyte adhesions as those observed in humans who succumb after infection with *Plasmodium falciparum*.[8] Therefore, results from this animal model may help in understanding the infection of humans by *P. falciparum*. The microcirculation of the hamster can be studied in the awake condition using a dorsal chamber window allowing the chronic and noninvasive observation of arterioles, venules, and capillaries throughout the entire time course of the disease. Furthermore, microvascular pO_2 levels can be assessed optically using the phosphorescence quenching technique,[9,10] providing data on intravascular, perivascular, and interstitial pO_2 values required for characterizing the microvascular oxygen distribution. Thus, this technique provides a means for extending previous acute microvascular studies of severe malaria in the hamster cheek pouch model[8] and investigating hemodynamic and tissue changes during the development of the disease, assuming that its micro-

Supported by grant AI40667 (to H.C.V.), the Bioengineering Research Partnership (grant R24-HL64395 to M.I.), and grants R01-HL62354 and R01-HL62318 (to M.I.).

Accepted for publication September 26, 2006.

Address reprint requests to Judith Martini, M.D., University of California–San Diego, Department of Bioengineering, 9500 Gilman Dr., La Jolla, CA 92093-0412. E-mail: judith.martini@med.uni-jena.de.

vascular pathologies are systemic and common to all tissues.

Herein, we report dynamic changes in the microcirculation of the hamster window chamber during infection with *P. berghei* in terms of vessel diameter, red blood cell (RBC) velocity, blood flow, and number of perfused capillaries (functional capillary density, FCD). We also test the hypothesis whether the sequestration of parasitized red blood cells (PRBCs) leads to the proposed decrease in microvascular blood flow and subsequent lowering of tissue oxygenation by measuring pO_2 levels in arterioles, venules, and the tissue.

Materials and Methods

Animal Preparation

Microcirculation investigations were performed in 55- to 65-g male Syrian golden hamsters (Charles River Laboratories, Boston, MA). Animal handling and care were provided following the procedures outlined in the Guide for the Care and Use of Laboratory Animals (National Research Council, 1996). The study was approved by the local animal subjects committee. The window chamber model is widely used for microvascular studies in the unanesthetized state, and the complete surgical technique is described in detail elsewhere.[11,12] Three days after infection with *P. berghei*, hamsters were prepared for chamber implantation with a 50 mg/kg i.p. injection of pentobarbital sodium anesthesia. After hair removal, sutures were used to lift the dorsal skin away from the animal, and one frame of the chamber was positioned on the animal's back. A chamber consisted of two identical titanium frames with a 15-mm circular window. With the aid of backlighting and a stereomicroscope, one side of the skinfold was removed after the outline of the window until only a thin layer of retractor muscle and the intact subcutaneous skin of the opposing side remained. Saline and then a cover glass were placed on the exposed skin held in place by the other part of the chamber. The intact skin of the other side was exposed to the ambient environment. The animal was allowed to recover for 3 days before daily microscopic observations were started.

Three animals were additionally equipped with an arterial catheter (PE-50) that was implanted in the carotid artery. The catheter was filled with a heparinized saline solution (30 IU/ml) to ensure patency for the entire time of observation. The catheter was tunneled under the skin and exteriorized at the dorsal side of the neck where it was attached to the chamber frame with tape.

Experimental Groups

Experiments were performed in four animals groups: 1) *P. berghei*-infected group ($n = 11$); 2) *P. berghei*-infected group with oxygen measurements ($n = 5$); 3) uninfected oxygen control group ($n = 5$); and 4) *P. berghei*-infected animals with an arterial catheter for measurements of systemic parameters ($n = 3$).

Infections of Hamsters

Hamsters (body weight 35 to 40 g) were injected intraperitoneally with 1.5×10^7 *P. berghei* parasitized erythrocytes obtained from a source animal infected by injection of frozen parasitized erythrocyte stabilate as described.[13] Animals were housed in microisolator cages and provided water and food *ad libitum*. Parasitemia levels were assessed on days 4, 6, 8, and 10 after the infection by counting the number of infected red blood among 200 and 1000 erythrocytes in Giemsa-stained thin blood films. Animals were scored for clinical signs of experimental severe malaria every day after the infection by determining their appearance (eg, breathing and ruffled fur). Day 7 after infection was chosen as the earliest observation day since animals showed mild depression beginning on days 6 to 7. In these series of experiments, all hamsters were sacrificed at the end of the experiment on day 10 since the *P. berghei*-infected animals showed severe clinical signs of experimental severe malaria.

Systemic Parameters

Surgical implantation of an arterial catheter in three infected hamsters allowed the measurement of blood gasses (pH, pO_2, pCO_2, and base excess), hematocrit (Hct), hemoglobin (Hb), mean arterial blood pressure, and heart rate on days 4, 6, 8, and 10 after the infection with *P. berghei*. Measurements of mean arterial blood pressure and heart rate were made by placing the animals in a restraining tube and recording blood pressure via a pressure transducer system (MP 150; Biopac System, Santa Barbara, CA). Measurements were recorded for 30 minutes, after the animals were fully adjusted to the tube environment and did not show any signs of discomfort. Hct was measured from centrifuged arterial blood samples taken in heparinized capillary tubes (Readacrit Centrifuge; Clay Adams, Division of Becton-Dickinson, Parsippany, NJ). Hb content was determined spectrophotometrically from a single drop of blood (B-Hemoglobin; Hemocue, Stockholm, Sweden). Arterial blood was collected in heparinized glass capillaries (0.05 ml) from the carotid catheter and immediately analyzed for PaO_2, $PaCO_2$, pH, and base excess (Blood Chemistry Analyzer 248; Bayer, Norwood, MA).

Assessment of Microcirculatory Parameters

Repeated microvascular measurements of vessel diameter, RBC velocity, and blood flow were made on the same sites from day 7 until day 10 after the infection with *P. berghei*. The anesthetized animals were placed in a restraining tube every day and given 30 to 60 minutes to adjust to the tube environment before measurements were taken. The tube was then attached to the microscopic stage of a transillumination intravital microscope (BX51WI; Olympus, New Hyde Park, NY). The tissue image was projected onto a charge-coupled device camera (no. 4815-2000; Cohu, San Diego, CA) connected to

a video cassette recorder (AG-7355; Panasonic, Tokyo, Japan) and viewed on a Sony monitor (PMV-1271Q; Sony, Tokyo, Japan). Measurements were made using a 40× (LUMPFL-WIR, NA 0.8; Olympus) water immersion objective. Sites of investigation were selected on day 7 to provide different locations (either arteriole or venule) throughout the microvascular network. The same sites of measurements were followed throughout the experiments so that comparison could be made directly to measurements of previous days.

RBC velocity in arterioles and venules was measured on-line by using the photodiode/cross-correlator system (Photo Diode/Velocity Tracker Model 102 B; Vista Electronics, San Diego, CA).[14] A video image-shearing method was used to measure vessel diameter.[15] The centerline velocity was corrected according to vessel size to obtain the mean RBC velocity (V).[16] Blood flow was calculated from the measured values as $Q = V \times \pi (D/2)^2$.

The same sites of investigation chosen for measurements of vessel diameter, RBC velocity, and blood flow were investigated every day for the appearance of parasitized RBCs (PRBCs). PRBCs can be easily identified in arterioles and venules of the chamber network because of the black appearance of the hemozoin granules within infected erythrocytes, the metabolic waste product of Hb digestion of the parasite.[17] Pictures of the same sites of investigation were taken every day to observe the development of aggregates of PRBCs throughout the time course of the infection.

Functional Capillary Density

FCD is the total length of RBC-perfused capillaries divided by the area of microscopic field of view.[18] Functional capillaries are defined as those capillary segments that have transit of at least one single RBC during a 30-second period. FCD was assessed in 10 successive microscopic fields (420 × 320 μm). Detailed mappings were made of the chamber vasculature to study the same capillary fields during the 4 consecutive days of observation.

Microvascular pO_2 Distribution

High-resolution noninvasive microvascular pO_2 measurements were made in five malaria-infected hamsters on day 10 after the infection and in five uninfected animals as a control group, using phosphorescence quenching microscopy.[10] Phosphorescence quenching microscopy is based on the oxygen-dependent quenching of phosphorescence emitted by an albumin-bound metalloporphyrin complex after pulsed light excitation. Phosphorescence quenching microscopy is independent of the dye concentration within the tissue and is used to measure both intravascular and extravascular pO_2 because the albumin-dye complex continuously extravasates into the interstitial tissue.[19,20] Interstitial pO_2 measurements have been found to be identical to simultaneous measurements made with recessed electrodes.[19] Tissue pO_2 was measured in regions between capillaries. The reported values are the average of several determinations in several animals. Phosphorescence quenching microscopy allows precise localization of the pO_2 measurements without subjecting the tissue to injury. The measurements provide detailed understanding of the microvascular oxygen distribution and show whether oxygen is delivered to interstitial areas.

The system setup has been described in detail elsewhere.[9,10] After inhalation anesthesia with isoflurane (AErrane; Baxter, Deerfield, IL), animals received a slow injection of 15 mg/kg palladium-meso-tetra (4-carboxyphenyl) porphyrin (concentration 10.1 mg/ml; Porphyrin Products, Inc., Logan, UT) in the retro-orbital plexus, which was allowed to circulate for 30 minutes. The 30-minute waiting time also guaranteed that the animals were fully awake at the time point when measurements were taken. The phosphorescence was excited by pulsed light (30 Hz, 4-μsecond duration) for a period of <5 seconds; the measurement site was microscopically vignetted by an adjustable slit. For intravascular measurements, an optical rectangular slit, ~5 × 35 μm, was positioned longitudinally within the vessel of interest. For interstitial tissue measurements, a 15 × 10-μm slit was placed in intercapillary spaces in regions void of large vessels. The phosphorescence decay curves were analyzed off line, using a standard single exponential least squares numerical fitting technique, and the resultant time constants were applied to the Stern-Volmer equation to calculate pO_2 using predetermined parameter corrected for this model.[9]

Oxygen Release

Oxygen release to the microcirculation was calculated by means of the following equation: O_2 release = Hct × $\Delta S_{A\text{-}V} \times \gamma \times$ MCHC × Q, where $\Delta S_{A\text{-}V}$ is the difference in O_2 saturation between arterioles and venules given by the O_2 dissociation curve, γ is the oxygen-carrying capacity of Hb at 100% saturation (1.34 ml of O_2/g of Hb), MCHC is the amount of Hb in g per unit RBC volumetric concentration (32.2 g/dl RBCs), and Q is the average flow (relative to baseline) through arteriolar and venular vessels on day 10 after the infection with *P. berghei.*

Analysis of Necrotic Cells

After assessing the blood flow, propidium iodide (5 mg/ml in 0.2 ml of phosphate-buffered saline) was injected intravenously and allowed to circulate for more than 0.5 hour. The microscope objective was focused at the selected vessel sites using transmitted and then digital epifluorescent images acquired of the propidium iodide-labeled cells using the Texas Red filter. The animals were then euthanized with an overdose of euthasol, and the same sites were analyzed ~0.5 hour later; there was no measurable blood flow at this time.

Table 1. Systemic Parameter Measurements

	Day 4	Day 6	Day 8	Day 10
Hct, %	48.3 ± 2.1	30.0 ± 0*	26.7 ± 1.6*	22.3 ± 2.1*
Hb, g/dl	14.8 ± 0.2	8.5 ± 0.4*	5.9 ± 0.1*	4.4 ± 0.4*
MAP, mm Hg	107 ± 8	87 ± 7	78 ± 12	79 ± 16
Heart rate, bpm	453 ± 22	443 ± 33	378 ± 44	313 ± 22†
PaO_2	65.5 ± 11	71.5 ± 4.5	65.3 ± 4.3	72 ± 7
$PaCO_2$	46.1 ± 2.9	53.9 ± 3.6	65.0 ± 4.7‡§	72.3 ± 7.5*§
pHa	7.36 ± 0.03	7.4 ± 0.03	7.33 ± 0.03	7.29 ± 0.05¶
BE, mmol/L	0.03 ± 1.44	8.03 ± 4.84	7.23 ± 4.06	7.57 ± 7.29

Values are means ± SD. Hct, systemic hematocrit; Hb, hemoglobin content of blood; MAP, mean arterial blood pressure; PaO_2, arterial partial O_2 pressure; $PaCO_2$, arterial partial pressure of CO_2; BE, base excess.
*$P < 0.001$ versus day 4.
†$P < 0.01$ versus day 4 and day 6.
‡$P < 0.01$ versus day 4.
§$P < 0.05$ versus day 6.
¶$P < 0.01$ versus day 6.

Statistical Analysis

Results are presented as means ± SD. Analysis of variance with the Statview program (SAS Institute, Cary, NC) was performed to compare statistically all measurements with a P value cutoff of 0.05.

Results

Systemic Parameters

Systemic parameters were measured in three animals with arterial catheters on days 4, 6, 8, and 10 after infection with *P. berghei* (Table 1). Mean arterial blood pressure decreased during the course of infection but did not reach significance. The heart rate, however, declined significantly ($P < 0.01$) on day 10 compared with days 4 and 6. Because the parasites replicated in and ruptured the erythrocytes, Hct and total Hb gradually decreased from day 4 to day 10 after infection, with all time points being statistically significantly different after day 4 ($P < 0.001$). Blood pH was not statistically different up to day 10, when it was significantly lower compared with days 4 and 6 (7.29 versus 7.36 and 7.40, $P < 0.05$). Base excess was unchanged from baseline throughout the time course of the entire experiment. $PaCO_2$ was significantly increased on days 8 and 10 compared with day 4 ($P < 0.01$ and $P < 0.001$, respectively) and compared with day 6 ($P < 0.05$ and $P < 0.01$, respectively). PaO_2 did not change from baseline during the entire observation period.

Microhemodynamics

We studied microvascular vessel diameter, RBC velocity, and blood flow in 11 hamsters infected with *P. berghei*; two animals were moribund on day 9, and the remaining nine animals were moribund on day 10. A total number of 40 arterioles and 52 venules were investigated on days 7, 8, and 9 after infection, and 34 arterioles and 41 venules were investigated on day 10; the lower number of vessels on day 10 was attributable to the fewer number of surviving animals on day 10. The microhemodynamic parameters in *P. berghei*-infected animals were compared with 31 arterioles and 26 venules in a group of healthy animals ($n = 5$).

Arterioles

Arterioles in infected animals exhibited slight (but not statistically significant) vasodilation compared with the uninfected control group (Figure 1A). Slight vasodilation was also observed between day 7 after infection and days 8, 9, and 10. At the individual vessel level, 16 arterioles of 34 exhibited vasodilation >10% between day 7 and day 10 after infection and 6 exhibited vasoconstriction of >10%. Arteriolar velocities increased significantly in the infected group on days 7, 8, and 9 after infection ($P = 0.0006$, 0.01, and 0.048, respectively) compared with the uninfected control group, but the changes were not significantly different from the control group on day 10 after the infection ($P = 0.14$) (Figure 1B).

Mean arteriolar blood flow was increased on all days compared with the control group (Figure 1C), a change that was statistically significant ($P = 0.02$) only on day 8 after the infection. Blood flows in the infected animals showed an increased SD (Figure 1B) attributable to decreased flow in some vessels resulting in increased flow in other vessels so that the overall flow into the tissue was maintained or slightly increased during the infection. In view of mass balance, decreased flow in certain vessels can only be compensated by a corresponding increase in flow in other vessels, which might be the cause for the wider flow range in malaria-infected animals. There were 17 arterioles that exhibited blood flow decreasing >20% between days 7 and 10 after infection and 12 with blood flow increasing >20%. Blood flow was not stopped in any of arterioles tested on day 10 of infection. The distribution of blood flow among vessels was very uneven (Figure 2). The histograms are characteristically skewed to the left on all observation days in infected animals and show a wider range of microvascular flows compared with the flow distribution of healthy hamsters (Figure 2).

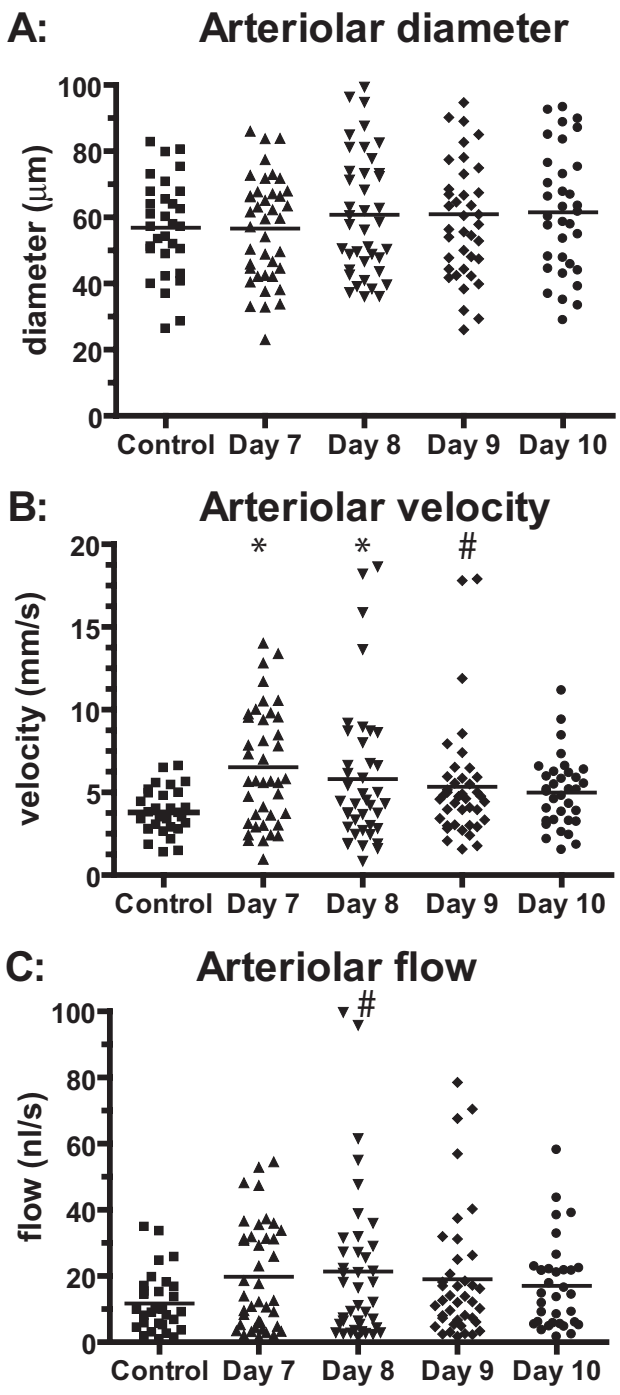

Figure 1. Absolute changes in arteriolar diameters, blood flow velocities, and blood flow throughout the time of the infection with *P. berghei* compared with an uninfected control group. **A:** Arterioles showed a slight but statistically not significant vasodilation compared with uninfected controls. **B:** Arteriolar velocities were significantly increased on days 7, 8, and 9 after the infection compared with controls. **C:** Arteriolar flows increased on all days compared with control animals, a finding that was significant only on day 8. $^{*}P < 0.005$; $^{\#}P < 0.05$.

Venules

Mean venular diameter (Figure 3A) was significantly increased on days 7, 8, and 10 after the infection compared with the control group of healthy hamsters (P = 0.02, 0.03, and 0.01, respectively). Diameters were still increased on day 9 but were not significantly different from the control group ($P = 0.07$). At the individual vessel level, 11 of 41 venules exhibited vasodilation of >10% between days 7 and 10 after infection and 14 exhibited vasoconstriction of >10%. Mean venular velocity (Figure 3B) was significantly increased on day 7 after the infection compared with healthy animals ($P = 0.01$). On days 8, 9, and 10, velocities were not significantly different from control animals. Velocities on day 10 were significantly lower than velocities on day 7 after the infection ($P = 0.008$). Mean venular blood flow (Figure 3C) was significantly ($P = 0.003$) increased on day 7 after the infection compared with the control group. Blood flows on days 8, 9, and 10 were slightly but not significantly increased compared with flow in uninfected controls. At the single venule level, 23 of the 41 venules exhibited blood flow lowered by >20% on day 10 after infection compared with days 7 and 12. One venule was completely occluded, and one vessel was almost occluded (98% reduction in blood flow). Two vessels exhibited more than a doubling of blood flow, presumably compensating for the low flow in other vessels. In parallel with the results in the arterioles, histograms of venular blood flow showed a wider range of microvascular flows compared with the control group (Figure 4).

Rolling and Adhesion of Leukocytes

Sixteen arterioles and 25 venules were analyzed at the same location from days 7 to 10 in terms of leukocyte rolling and firm adhesion to the vascular wall. Leukocyte rolling and adhesion did not occur in all investigated vessels. Of 16 investigated arterioles, only three exhibited rolling leukocytes: arteriole 1: one rolling leukocyte on day 8 after the infection; arteriole 2: seven rolling leukocytes on day 7 after the infection and no more rolling cells on the following days; and arteriole 3: one rolling leukocyte on day 9 after the infection. Only one arteriole showed one adhering leukocyte on day 9 after the infection with *P. berghei*.

Venules exhibited greater numbers of rolling and adherent leukocytes than arterioles, and a large variance of numbers of rolling and adhering leukocytes was observed in venules (Figure 5). Venules with no rolling or adhering leukocytes co-existed next to vessels with large numbers of leukocytes. Four single venules were chosen to demonstrate the patterns of variability in terms of leukocyte rolling and adhesion among different venules (Figure 5, A and C). Venule 1 exhibited high numbers of rolling leukocytes initially on day 7 and then no adhesion until the animal died on day 9 after infection; venule 2 exhibited no rolling leukocytes on days 7 and 8 after the infection, but marked rolling and adhesion late in the disease; venule 3 exhibited three rolling leukocytes only on day 10 after the infection when the animal was moribund; and venule 4 exhibited no leukocyte rolling or adhesion on any days after the infection with *P. berghei*. The summary of all rolling and adherent leukocytes in all venules indicates that leukocyte rolling and adhesion was

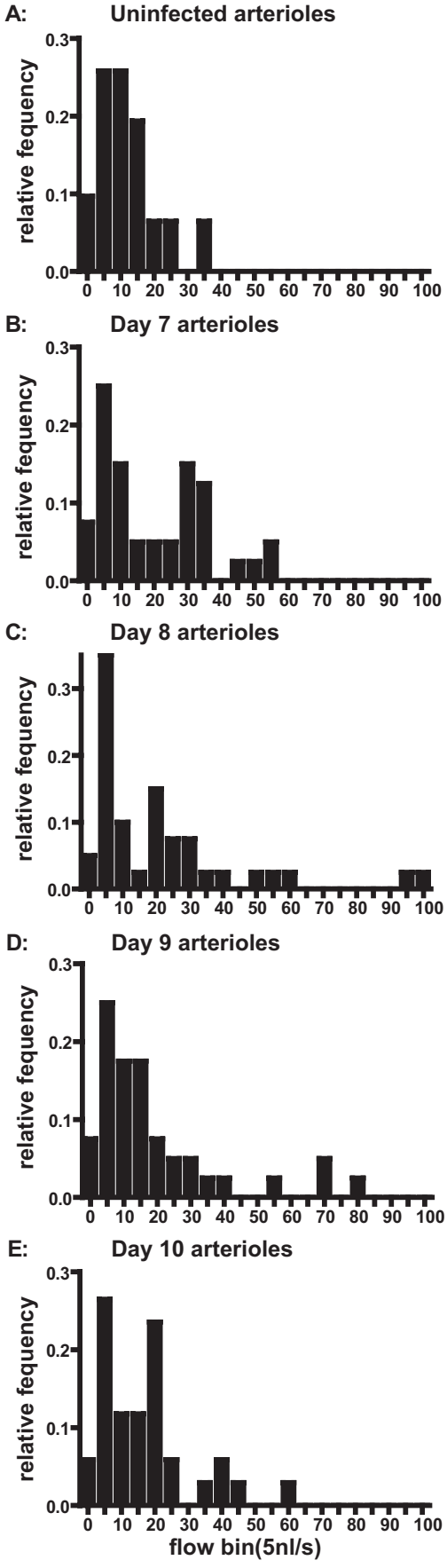

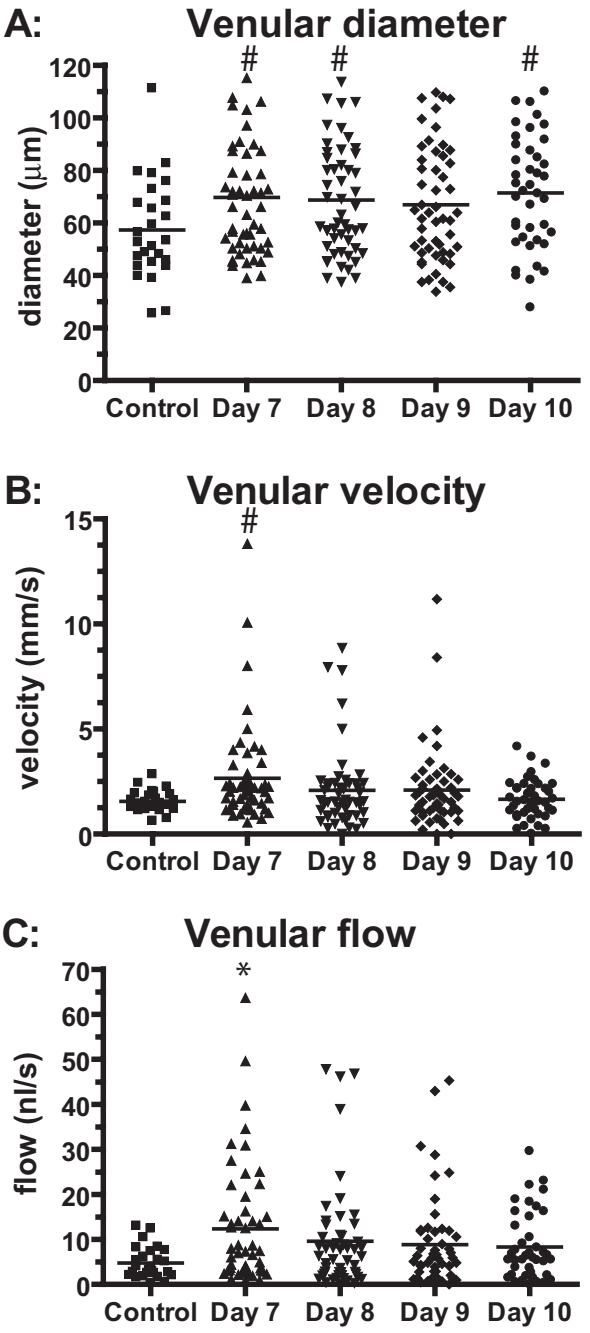

Figure 3. Absolute changes in venular diameter, blood flow velocities, and blood flow throughout time of the infection with *P. berghei* compared with an uninfected control group. **A:** Diameters were significantly increased on days 7, 8, and 10 after infection. **B:** Velocities were significantly increased on day 7 compared with control; velocities on day 10 were significantly decreased compared with day 7. **C:** Venular blood flow was significantly increased only on day 7 compared with uninfected controls. $^{*}P < 0.005$ versus control; $^{\#}P < 0.05$ versus control.

Figure 2. Microvascular flow distribution for arterioles on days 0 (uninfected, **A**), 7 (**B**), 8 (**C**), 9 (**D**), and 10 (**E**) after the infection with *P. berghei.*

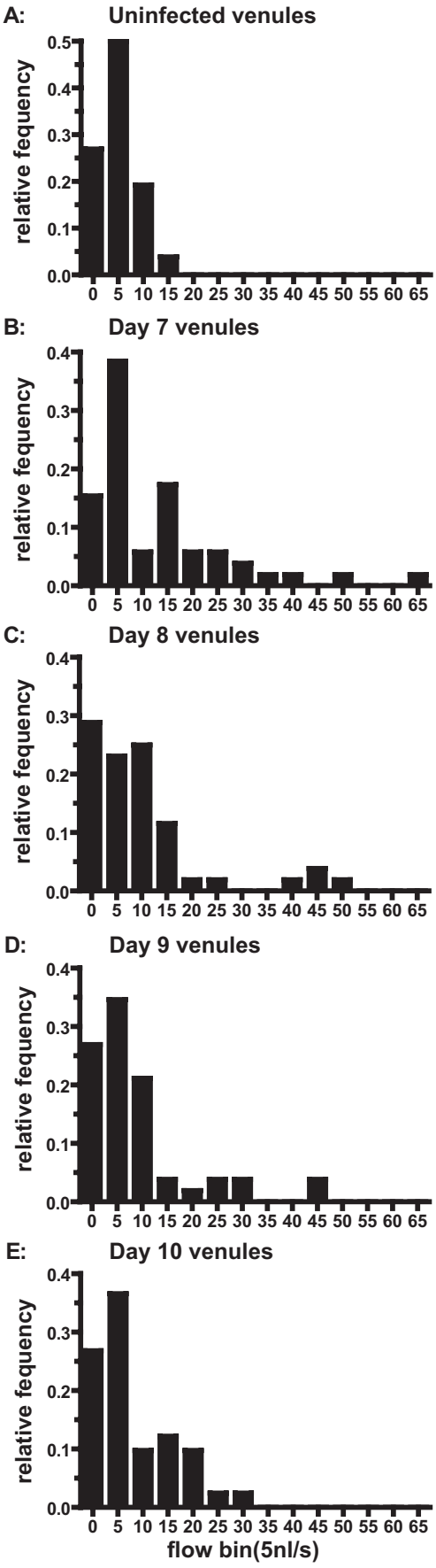

increased by infection but was not pronounced with large numbers of adherent leukocytes occluding blood flow (Figure 5, B and D).

Adhesion of PRBCs

Adhesion of PRBCs was observed in venules (Figure 6) as well as in arterioles and was observed to be a dynamic process: we found adhesion of single PRBCs as well as formation of aggregates consisting of more than two PRBCs. Some aggregates increased in size because of adhesion of additional PRBCs throughout time, and other aggregates were found to disintegrate over time, presumably because the local microvascular flow was strong enough to remove single cells or parts of the aggregate.

Of 16 investigated arterioles, seven exhibited adhesion of single PRBCs: arteriole 1: three PRBCs on day 10 after infection; arteriole 2: one PRBC on day 9; arteriole 3: one PRBC on day 8; arteriole 4: two PRBCs on day 9; arteriole 5: two PRBCs on days 8 and four on day 10; arteriole 6: two PRBCs on day 8; and arteriole 7: one PRBC on day 8 after infection. Only four arterioles showed formation of PRBC aggregates during the infection: arteriole 1: one aggregate on days 8 and 9; arteriole 2: one aggregate on day 10 when the animals was moribund; arteriole 3: two aggregates on day 9; and arteriole 4: two aggregates on day 8 after infection.

The process of adhesion of single PRBCs as well as adhesion of PRBC aggregates in venules is shown in Figure 6. Analysis of PRBC adhesion in vessels indicated similar variability as observed for leukocyte adhesion (Figure 6, A and C). A summary of all of the investigated venules (Figure 6, B and D) supports the variability of adhesion of single PRBCs and aggregates of PRBCs. Figure 7 shows the image of a small collecting venule merging into a larger venule from day 7 until day 10 after infection and documents pictorially the described variability of PRBC adhesion and aggregate formation.

Functional Capillary Density (FCD)

Malaria infection caused FCD to be significantly lower on all observation days compared with the control group ($P < 0.0001$) (Figure 8). In addition, the FCD declined as the infection progressed, suggesting that FCD may be an indicator of a poor prognosis. The FCD on days 9 and 10 were significantly less compared with day 7 (day 9 versus day 7: $P = 0.02$; day 10 versus day 7: $P = 0.002$).

Number of Necrotic Cells

No cells labeled with propidium iodide were detected in the focal plane of the selected vessels in live animals. However, cells were brightly fluorescent after the animal

Figure 4. Microvascular flow distribution for venules on days 0 (uninfected, **A**), 7 (**B**), 8 (**C**), 9 (**D**), and 10 (**E**) after the infection with *P. berghei*.

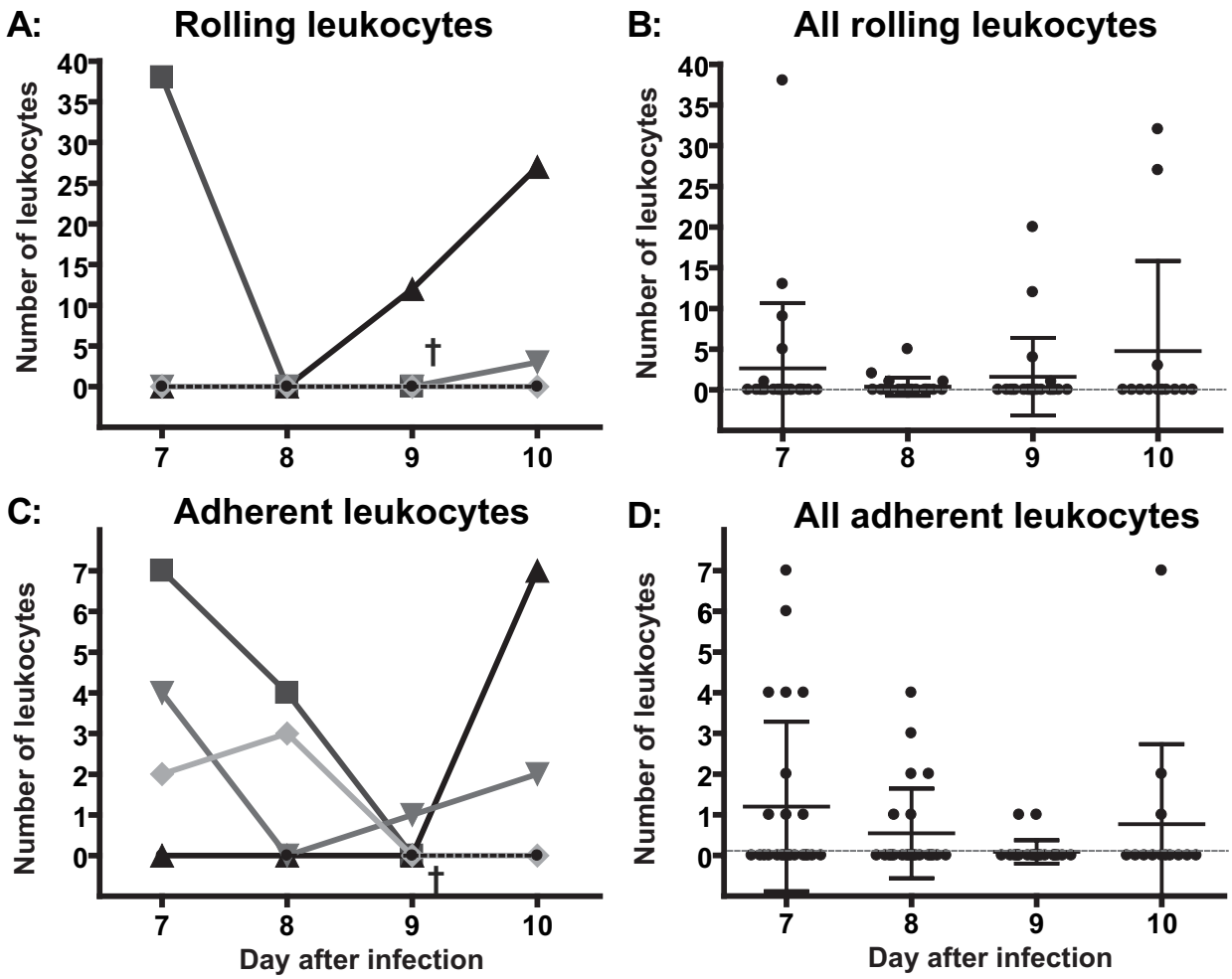

Figure 5. Rolling and adhesion of leukocytes in venules. **A** and **C:** Four single venules are chosen to demonstrate the variability in terms of leukocyte rolling and adhesion among different venules. **B** and **D** show rolling and adhesion of leukocytes in all investigated venules. †Death of the animal.

had been euthanized, indicating that sufficient fluorochrome was present to actually label necrotic cells.

Microvascular Oxygen Distribution

Microvascular oxygen measurements were taken on day 10 after the infection when the animals were moribund in 19 arterioles and 22 venules and compared with oxygen values of uninfected animals.

Arterioles

Intravascular oxygen tension was not significantly ($P = 0.7$) different from uninfected control animals (Figure 9A), perivascular oxygen tensions were significantly decreased compared with control ($P < 0.0001$), and oxygen gradients were significantly increased compared with uninfected control animals ($P < 0.0001$).

Venules

Intravascular oxygen tensions were significantly lower compared with uninfected animals (Figure 9B, $P < 0.0001$). Perivascular oxygen tensions as well as oxygen gradients were also significantly lower compared with uninfected animals ($P < 0.0001$ and, $P = 0.01$, respectively).

Tissue Oxygen

Tissue oxygen tension was significantly lower in infected animals compared with control animals (Figure 10; $P < 0.0001$). However, oxygen tensions did not reach levels considered to be lethal (3 mm Hg).

Oxygen Release

Oxygen release was 4.7 ml/second in infected animals and 4.9 ml/second in uninfected control animals. This slight decrease in oxygen release in *P. berghei*-infected animals was not statistically significant.

Discussion

The principal finding of our study is that FCD was ~50% lower compared with an uninfected control group on day

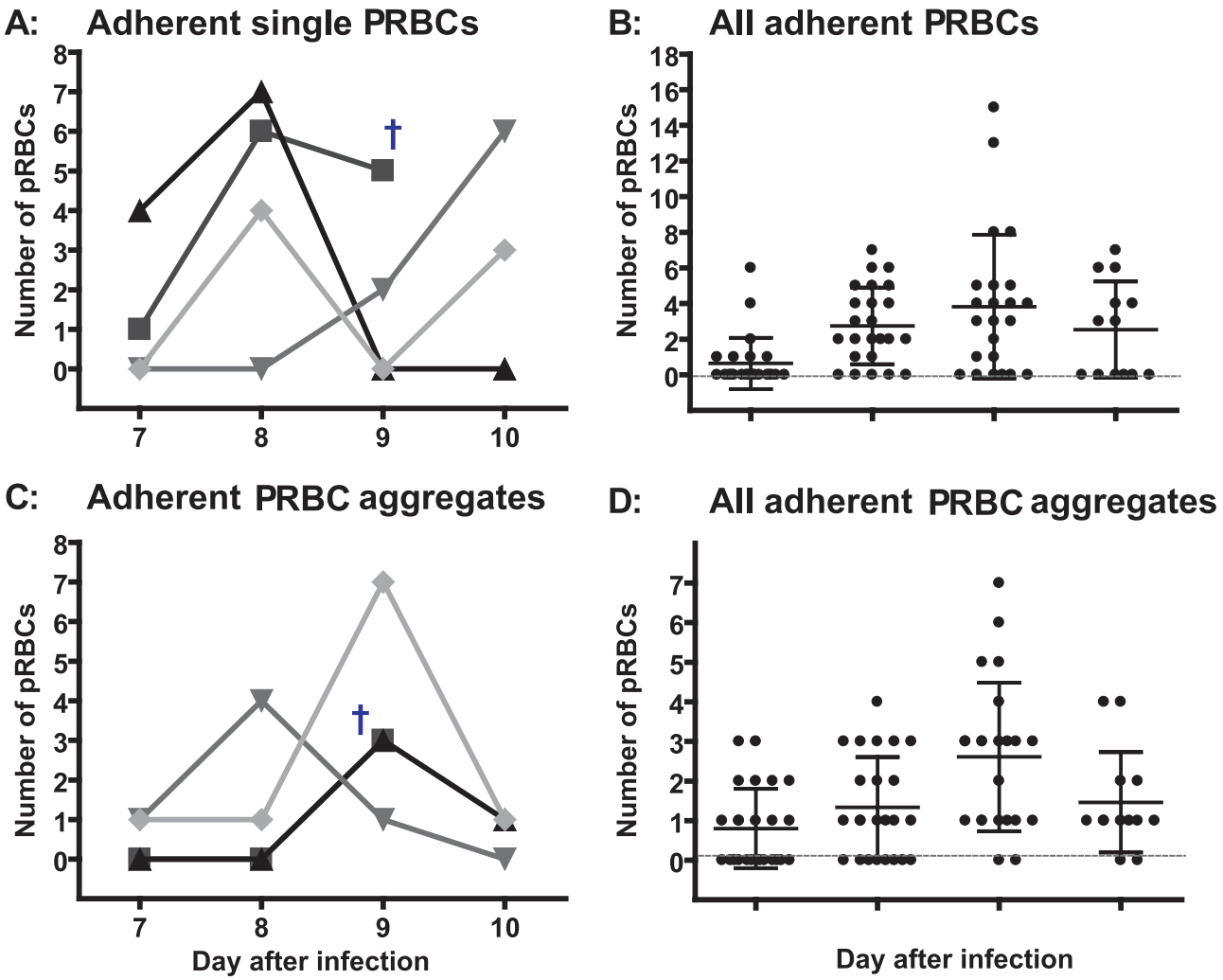

Figure 6. Adhesion of single PRBCs and formation of PRBC aggregates in venules. **A** and **C:** The variability of single PRBC adhesion and aggregate formation is shown on the level of four single venules. **B** and **D:** The results of all investigated venules. †Death of the animal.

7 after the infection and decreased further to ~20% of control on day 10 after the infection. Capillaries mainly appeared as empty tubes with erythrocytes appearing to be occasionally trapped inside. This early presentation of decreased FCD and its subsequent decrease during the course of infection suggest that FCD may be a new indicator of poor prognosis and for the initiation of adjunct therapy. Indeed, Rivers[21] has proposed that monitoring of FCD during sepsis may be beneficial, with marked decreases in FCD signaling the onset of severe disease. Although other mechanisms such as tissue edema and cell aggregates may contribute to decreased FCD, we hypothesize that loss of RBC flexibility, which is a well-known phenomenon occurring during malaria infection,[22–25] hindered erythrocytes from entering the narrow capillary lumen (~8 μm)[26] and contributed to the drastic decrease in FCD. In support of this contention, Dondorp and colleagues[22] has reported that RBC deformability is impaired during severe *P. falciparum* malaria in humans and is a predictor of severe malaria. The decreased RBC deformability may be attributable to the presence of parasite-derived proteins in the RBC membranes increasing its stiffness and the presence of a rigid parasite within the RBC, increasing its internal viscosity. The production of reactive oxygen species is also believed to render the uninfected RBCs more rigid, but the mechanisms remain to be determined. The decreased FCD during severe malaria may hinder removal of waste products and possibly oxygen delivery to the tissue.

Another factor proposed to affect removal of waste products from tissue and oxygen delivery to the tissue is the adherence of cell aggregates made predominantly of PRBCs primarily in postcapillary venules. In our model, these cell aggregates were dynamic, moving from their original location presumably when either blood flow was strong enough to produce the necessary shear forces or the underlying PRBCs lysed during parasite replication. The movement of cell aggregates was especially evident in arterioles, where blood flows are higher compared with venules. In general, regions with low arteriolar flow tended to have lower FCD.

In the present study, we observed sequestration of PRBCs *in vivo*, which takes place in venules and in arterioles. However, total occlusion of blood vessels in the

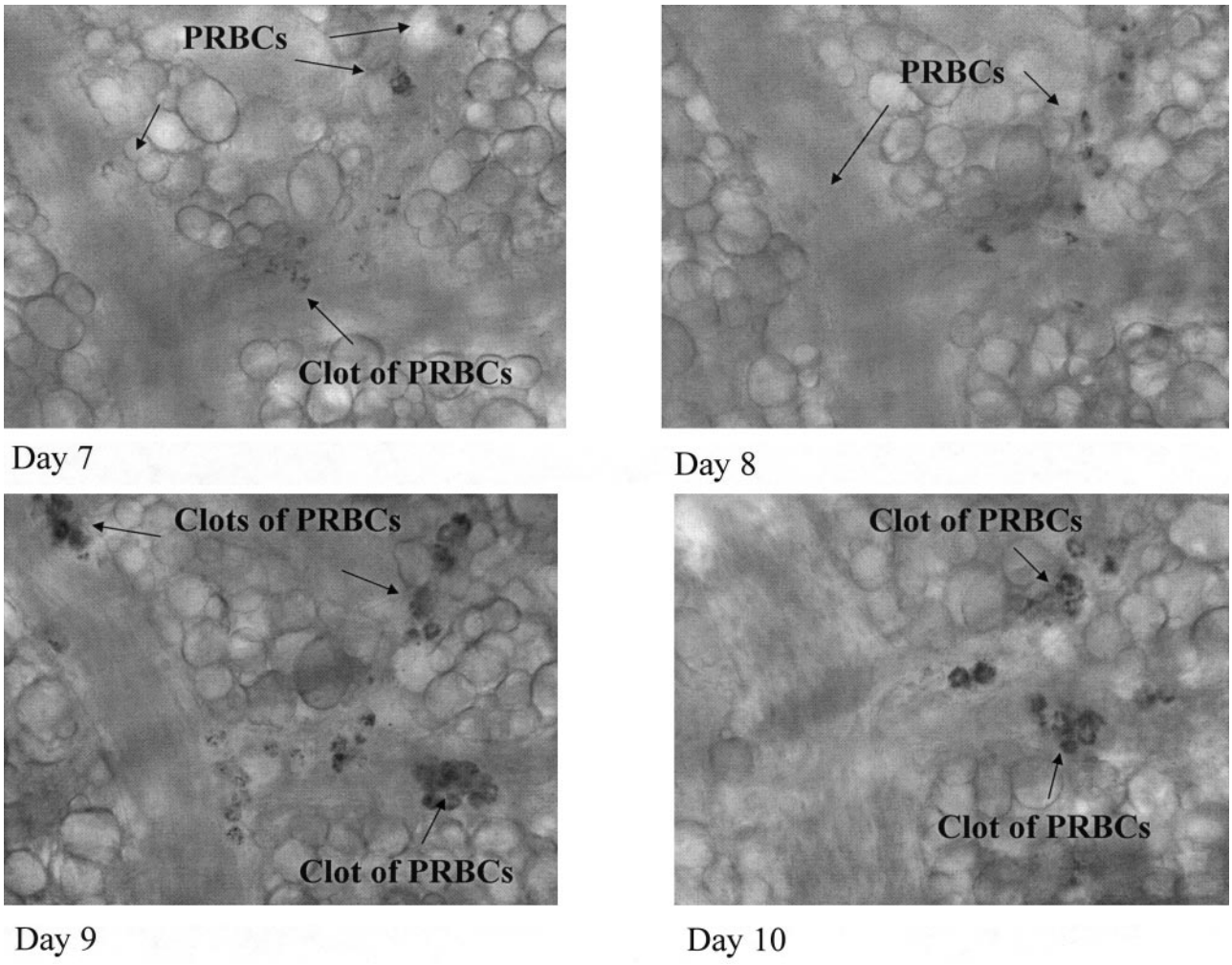

Figure 7. Images of aggregates mainly consisting of PRBCs in venules of the microcirculation of the hamster window chamber. Aggregate formation was found to be a highly dynamic process.

microcirculation was rare. Blood flow was heterogeneous: vessels with low flow (50% and lower than the control group) co-existed next to vessels with very high blood flow (double the flow of the control group), resulting in a high dispersion of blood flow values. This fact resulted in no statistical significance for blood flow values in infected animals compared with the control group. Blood flow at the sites of cell aggregates was mostly unimpaired, suggesting that other factors such as FCD determines flow in the network of vessels.

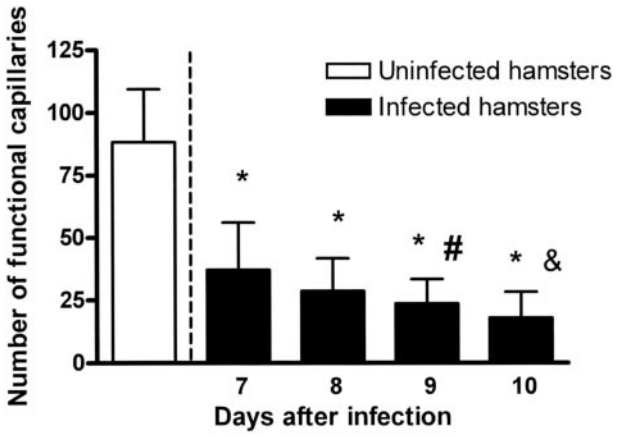

Figure 8. FCD during infection with *P. berghei*. FCD gradually decreased during the infection, reaching levels 20% of control on day 10 after the infection. This finding reflects a highly disturbed microvascular function. $^{*}P < 0.005$ versus day 7; $^{\#}P < 0.05$ versus control; $^{\&}P < 0.005$ versus day 7.

These findings of cell aggregates in postcapillary venules are consistent with observations made on brain slides obtained from patients who died of severe malaria, suggesting microvascular failure, generally attributed to the mechanical obstruction of microvessels by PRBCs and mononuclear cells, presumed to cause decreased microvascular blood flow and lowering of oxygen release to tissues.[5,6,23,24,27,28] However, these tissue slides represent a nonphysiological situation compared with the *in vivo* conditions. The present study shows that sequestration of PRBCs does not cause blood flow to decrease. This only occurs if a blood vessel is 100% occluded.

Functionally, the significant decrease in FCD found with progression of malaria is the most critical microvascular pathology that ultimately leads to organ failure. FCD

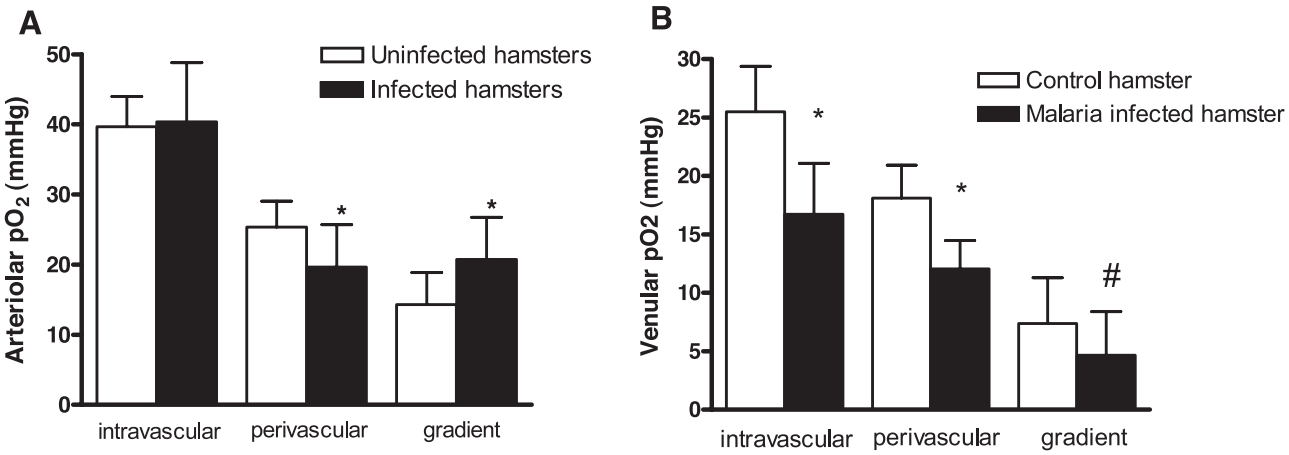

Figure 9. Microvascular oxygen distribution for arterioles and venules on day 10 after infection with *P. berghei* compared with uninfected controls. Arterioles: perivascular oxygen and oxygen gradients were significantly lower in infected compared with uninfected animals (**A**). Venules: intravascular, perivascular, and oxygen gradients across the vascular wall were significantly decreased in infected compared with uninfected hamsters (**B**). $^{*}P < 0.005$ versus control; $^{\#}P < 0.05$ versus control.

is a parameter reflecting tissue perfusion and is an indicator of tissue viability.[26] Kerger and colleagues[29] showed that after 4 hours of hemorrhagic shock, FCD was the only microvascular parameter that distinguished surviving from nonsurviving animals. Whereas in surviving animals FCD levels were maintained at ~30% compared with baseline, in nonsurviving animals FCD decreased to 0% of baseline. Cabrales and colleagues[30,31] studied hemorrhagic shock and resuscitation in the hamster window chamber and showed that FCD significantly increased from shock levels after successful resuscitation. Tsai and colleagues[18] demonstrated that extreme hemodilution to a systemic Hct of 11% could only be tolerated if blood viscosity was elevated using high-viscosity plasma expanders that maintained FCD close to baseline values (~80% of baseline). These studies demonstrate that maintenance of physiological levels of FCD is crucial for tissue survival.

FCD levels found in animals infected with *P. berghei* are clearly in a highly pathological range, being similar to animals that underwent severe hemorrhagic shock. Loss of FCD in shock coincides with severe derailment of acid base balances (eg, acidic pH, negative base excess, and low bicarbonate)[29–33]; however, malaria-infected hamsters did not show major disturbances of acid base status. Metabolic acidosis and negative base excess are classical findings in cerebral malaria in humans, especially in children, and patients may present deep Kussmaul's breathing as a sign of respiratory distress.[34–36] The degree of metabolic acidosis (especially lactic acidosis) has been shown to be a strong indicator of poor outcome[6,37] as lactate concentrations are typically 1.5- to 2-fold higher in patients with a more severe disease progression.[37] However, in our study the only significant change in blood gasses was an increase in pCO_2 levels, whereas pH was only slightly decreased below physiological values in two of three animals, and base excess was slightly negative in only one of three animals. This discrepancy may be attributable to the relative insensitivity to acidosis of this animal species, which has a relatively higher blood buffer capacity[38] as a consequence of its adaptation to a fossorial environment of low oxygen and high carbon dioxide concentrations.[38,39] Nevertheless, the conclusion from this animal model regarding the contribution of PRBC sequestration to microcirculatory dysfunction should be relevant because it allows the chronic observation of the microcirculation throughout the entire duration of the disease without influences of anesthesia.[40–42]

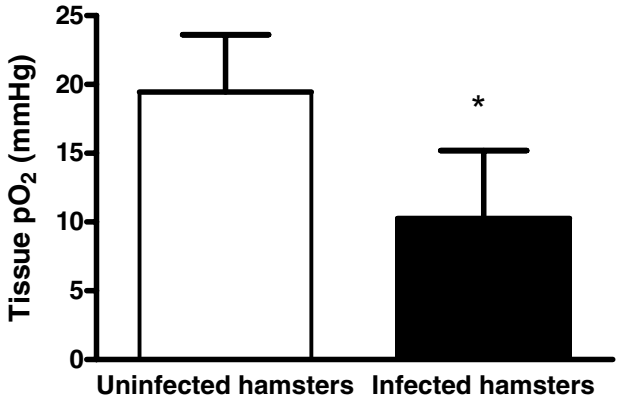

Figure 10. Tissue oxygen tensions in infected and uninfected animals. Infected animals showed significantly lower tissue oxygen tension compared with uninfected hamsters. However, tissue oxygen levels did not reach values considered to be lethal (~3 mm Hg). $^{*}P < 0.005$ versus control.

Since the early work of August Krogh,[43] it is believed that capillaries are the main source of oxygen for tissues. However, Duling and Berne[44] and later Swain and Pittman[45] reported that a significant fraction of the total tissue oxygen supply may be by diffusion from precapillary arterioles. Therefore, tissue oxygenation may not be the only important capillary function, and removal of metabolic waste products may be equally significant. Our results support this concept, showing that even though FCD is 20% of control before infected animals succumb to severe malaria, tissue oxygen, although significantly lower compared with control, did not reach levels considered to be lethal (~3 mm Hg) in this nonvital organ.

This was related to oxygen release in the microcirculation not being significantly lower in infected animals compared with uninfected controls (4.66 versus 4.86 ml/second, respectively). Although Hct, and therefore oxygen-carrying capacity, was significantly reduced in infected animals on day 10 after the infection, arteriolar and venular blood flows were not significantly lower compared with the uninfected control group, which maintained oxygen release close to control levels. Whether the decline of FCD is similar in the brain and whether a similar magnitude of tissue oxygenation decline occurs in the brain remains to be determined.

This finding is in contrast with the mechanical obstruction or sequestration hypothesis, indicating that mechanical obstruction of microvessels with PRBCs decreases blood flow and therefore oxygen release to tissues.[1,17] Our results suggest a more complex situation, showing that even though there is adherence of PRBCs to microvessels, particularly in venules, microvascular flow is generally maintained presumably through vessels which assume shunt-like functions. These shunts allow the transmission of arteriolar flow to the venular portion of the microvascular network even though FCD was reduced to 20% of control values. Consequently, oxygen supply to tissues is only moderately impaired as shown in our study.

According to the mechanical obstruction hypothesis, tissue hypoxia would be the fatal event in severe malaria. Given the significance of FCD for maintaining tissue viability in general, not exclusively related to oxygen supply, it would seem that loss of FCD rather than tissue hypoxia is the key event in severe malaria. Furthermore, it seems that FCD is the only microvascular parameter that measures the disease severity during malaria infection, and consequently, it may be a biomarker for the development of disease.

Arterioles showed significantly elevated oxygen gradients across the vascular wall compared with uninfected animals. Vascular oxygen gradients are an indicator for oxygen consumption of the vessel wall, which consists of endothelial and smooth muscle cells.[46] A significant amount of oxygen is consumed by these cells to maintain vasoconstriction and produce vasoactive transmitters, a process that can lead to severe tissue hypoxia.[47] The significantly increased arteriolar oxygen gradients in our study is most likely caused by increased oxygen consumption of endothelial cell rather than smooth muscle, because vasodilation, which is a passive, nonoxygen-consuming process,[48] was prevalent.

Endothelial cells, especially cerebral endothelial cells, express and up-regulate cyclooxygenase 2 mRNA in response to malaria infection.[49–51] Grau and colleagues[52–54] identified tumor necrosis factor (cachectin) as one of the most important cytokines associated with human and murine cerebral malaria and it has been shown[55] that tumor necrosis factor up-regulates the expression of intercellular adhesion molecule 1 (ICAM-1/CD54), which represents an important ligand for infected RBCs and mononuclear cells on brain endothelial cells. These and possibly other synthesis processes might increase oxygen consumption of endothelial cells and could account for the increased arteriolar oxygen gradients found in our model.

In summary, tissue hypoxia after mechanical obstruction of microvessels with PRBCs has generally been considered to be the key event during severe malaria. However, in this study we showed that *P. berghei*-induced severe malaria only leads to mild tissue hypoxia in the hamster window model because of conservation of microvascular flow through vessels that assume shunt-like functions. The most important microvascular pathology was the decrease of FCD to 20% compared with uninfected animals on day 10 after the infection, which corresponds to FCD levels of animals that underwent severe hemorrhagic shock[29,32,33] and that do not survive. We therefore conclude that the loss of functional capillaries, an effect independent of tissue oxygenation, rather than low tissue oxygenation is a hallmark of severe malaria.

Acknowledgments

We thank Froilan P. Barra and Cynthia Walser for the surgical preparation of the animals.

References

1. Idro R, Jenkins NE, Newton CR: Pathogenesis, clinical features, and neurological outcome of cerebral malaria. Lancet Neurol 2005, 4:827–840
2. Day NP, Phu NH, Mai NT, Chau TT, Loc PP, Chuong LV, Sinh DX, Holloway P, Hien TT, White NJ: The pathophysiologic and prognostic significance of acidosis in severe adult malaria. Crit Care Med 2000, 28:1833–1840
3. Marsh K, Forster D, Waruiru C, Mwangi I, Winstanley M, Marsh V, Newton C, Winstanley P, Warn P, Peshu N, Pasvol G, Snow R: Indicators of life-threatening malaria in African children. N Engl J Med 1995, 332:1399–1404
4. Waller D, Krishna S, Crawley J, Miller K, Nosten F, Chapman D, ter Kuile FO, Craddock C, Berry C, Holloway PA, Brewster D, Greenwood BM, White NJ: Clinical features and outcome of severe malaria in Gambian children. Clin Infect Dis 1995, 21:577–587
5. Berendt AR, Tumer GD, Newbold CI: Cerebral malaria: the sequestration hypothesis. Parasitol Today 1994, 10:412–414
6. Miller LH, Baruch DI, Marsh K, Doumbo OK: The pathogenic basis of malaria. Nature 2002, 415:673–679
7. Planche T: Malaria and fluids—balancing acts. Trends Parasitol 2005, 21:562–567
8. Franz DR, Lee M, Seng LT, Young GD, Baze WB, Lewis Jr GE: Peripheral vascular pathophysiology of Plasmodium berghei infection: a comparative study in the cheek pouch and brain of the golden hamster. Am J Trop Med Hyg 1987, 36:474–480
9. Kerger H, Groth G, Kalenka A, Vajkoczy P, Tsai AG, Intaglietta M: pO_2 measurements by phosphorescence quenching: characteristics and applications of an automated system. Microvasc Res 2003, 65:32–38
10. Torres Filho IP, Intaglietta M: Microvessel pO_2 measurements by phosphorescence decay method. Am J Physiol 1993, 265:H1434–H1438
11. Colantuoni A, Bertuglia S, Intaglietta M: Quantitation of rhythmic diameter changes in arterial microcirculation. Am J Physiol 1984, 246:H508–H517
12. Endrich B, Asaishi K, Götz A, Messmer K: Technical report: a new chamber technique for microvascular studies in unanaesthetized hamsters. Res Exp Med 1980, 177:125–134
13. Hoffmann EJ, Weidanz WP, Long CA: Susceptibility of CXB recombinant inbred mice to murine plasmodia. Infect Immun 1984, 43:981–985
14. Intaglietta M, Silverman NR, Tompkins WR: Capillary flow velocity

measurements in vivo and in situ by television methods. Microvasc Res 1975, 10:165–179
15. Intaglietta M, Tompkins WR: On-line microvascular blood cell flow velocity measurement by simplified correlation technique. Microvasc Res 1972, 4:217–220
16. Lipowsky HH, Zweifach BW: Application of the "two-slit" photometric technique to the measurement of microvascular volumetric flow rates. Microvasc Res 1978, 15:93–101
17. Rogerson SJ, Grau GE, Hunt NH: The microcirculation in severe malaria. Microcirculation 2004, 11:559–576
18. Tsai AG, Friesenecker B, McCarthy M, Sakai H, Intaglietta M: Plasma viscosity regulates capillary perfusion during extreme hemodilution in hamster skin fold model. Am J Physiol 1998, 275:H2170–H2180
19. Buerk DG, Tsai AG, Intaglietta M, Johnson PC: In vivo hamster skin fold tissue pO_2 measurements by phosphorescence quenching and recessed pO_2 microelectrodes are in agreement. Microcirculation 1998, 5:219–225
20. Tsai AG, Friesenecker B, Mazzoni MC, Kerger H, Buerk DG, Johnson PC, Intaglietta M: Microvascular and tissue oxygen gradients in the rat mesentery. Proc Nat Acad Sci USA 1998, 95:6590–6595
21. Rivers EP: Early goal-directed therapy in severe sepsis and septic shock: converting science to reality. Chest 2006, 129:217–218
22. Dondorp AM, Angus BJ, Hardeman MR, Chotivanich KT, Silamut K, Ruangveerayuth R, Kager PA, White NJ, Vreeken J: Prognostic significance of reduced red blood cell deformability in severe falciparum malaria. Am J Trop Med Hyg 1997, 57:507–511
23. Dondorp AM, Nyanoti M, Kager PA, Mithwani S, Vreeken J, Marsh K: The role of reduced red cell deformability in the pathogenesis of severe falciparum malaria and its restoration by blood transfusion. Trans R Soc Trop Med Hyg 2002, 96:282–286
24. Dondorp AM, Pongponratn E, White NJ: Reduced microcirculatory flow in severe falciparum malaria: pathophysiology and electron-microscopic pathology. Acta Trop 2004, 89:309–317
25. Glenister FK, Coppel RL, Cowman AF, Mohandas N, Cooke BM: Contribution of parasite proteins to altered mechanical properties of malaria-infected red blood cells. Blood 2002, 99:1060–1063
26. Tsai AG, Friesenecker B, Intaglietta M: Capillary flow impairment and functional capillary density. Int J Microcirc Clin Exp 1995, 15:238–243
27. Miller LH, Usami S, Chien S: Alteration in the rheologic properties of Plasmodium knowlesi-infected red cells. A possible mechanism for capillary obstruction. J Clin Invest 1971, 50:1451–1455
28. Pettersson F, Vogt AM, Jonsson C, Mok BW, Shamaei-Tousi A, Bergstrom S, Chen Q, Wahlgren M: Whole-body imaging of sequestration of Plasmodium falciparum in the rat. Infect Immun 2005, 73:7736–7746
29. Kerger H, Saltzman DJ, Menger MD, Messmer K, Intaglietta M: Systemic and subcutaneous microvascular pO_2 dissociation during 4-h hemorrhagic shock in conscious hamsters. Am J Physiol 1996, 270:H827–H836
30. Cabrales P, Intaglietta M, Tsai AG: Increase plasma viscosity sustains microcirculation after resuscitation from hemorrhagic shock and continuous bleeding. Shock 2005, 23:549–555
31. Cabrales P, Nacharaju P, Manjula BN, Tsai AG, Acharya SA, Intaglietta M: Early difference in tissue pH and microvascular hemodynamics in hemorrhagic shock resuscitation using polyethylene glycol-albumin- and hydroxyethyl starch-based plasma expanders. Shock 2005, 24:66–73
32. Kerger H, Tsai AG, Saltzman DJ, Winslow RM, Intaglietta M: Fluid resuscitation with O_2 vs. non-O_2 carriers after 2 h of hemorrhagic shock in conscious hamsters. Am J Physiol 1997, 272:H525–H537
33. Kerger H, Waschke KF, Ackern KV, Tsai AG, Intaglietta M: Systemic and microcirculatory effects of autologous whole blood resuscitation in severe hemorrhagic shock. Am J Physiol 1999, 276:H2035–H2043
34. English M, Sauerwein R, Waruiru C, Mosobo M, Obiero J, Lowe B, Marsh K: Acidosis in severe childhood malaria. QJM 1997, 90:263–270
35. English M, Waruiru C, Amukoye E, Murphy S, Crawley J, Mwangi I, Peshu N, Marsh K: Deep breathing in children with severe malaria: indicator of metabolic acidosis and poor outcome. Am J Trop Med Hyg 1996, 55:521–524
36. Taylor TE, Borgstein A, Molyneux ME: Acid-base status in paediatric Plasmodium falciparum malaria. Q J Med 1993, 86:99–109
37. Newton CR, Valim C, Krishna S, Wypij D, Olola C, Agbenyega T, Taylor TE: The prognostic value of measures of acid/base balance in pediatric falciparum malaria, compared with other clinical and laboratory parameters. Clin Infect Dis 2005, 41:948–957
38. Holloway DA, Heath AG: Ventilatory changes in the golden hamster, Mesocricetus auratus, compared with the laboratory rat, Rattus norvegicus, during hypercapnia and/or hypoxia. Comp Biochem Physiol A 1984, 77:267–273
39. O'Brien JJ, Lucey EC, Snider GL: Arterial blood gases in normal hamsters at rest and during exercise. J Appl Physiol 1979, 46:806–810
40. Colantuoni A, Bertuglia S, Intaglietta M: Effects of anesthesia on the spontaneous activity of the microvasculature. Int J Microcirc Clin Exp 1984, 3:13–28
41. Colantuoni A, Bertuglia S, Intaglietta M: Microvessel diameter changes during hemorrhagic shock in unanesthesized hamsters. Microvasc Res 1985, 30:133–142
42. Kerger H, Saltzman DJ, Gonzales A, Tsai AG, van Ackern K, Winslow RM, Intaglietta M: Microvascular oxygen delivery and interstitial oxygenation during sodium pentobarbital anesthesia. Anesthesiology 1997, 86:372–386
43. Krogh A: The number and distribution of capillaries in muscle with the calculation of the oxygen pressure necessary for supplying the tissue. J Physiol 1919, 52:409–515
44. Duling BR, Berne RM: Longitudinal gradients in periarteriolar oxygen tension. A possible mechanism for the participation of oxygen in the local regulation of blood flow. Circ Res 1970, 27:669–678
45. Swain DP, Pittman RN: Oxygen exchange in the microcirculation of hamster cremaster muscle. Am J Physiol 1989, 256:H247–H255
46. Tsai AG, Johnson PC, Intaglietta M: Oxygen gradients in the microcirculation. Physiol Rev 2003, 83:933–963
47. Friesenecker B, Tsai AG, Dunser MW, Mayr AJ, Martini J, Knotzer H, Hasibeder W, Intaglietta M: Oxygen distribution in microcirculation after arginine vasopressin-induced arteriolar vasoconstriction. Am J Physiol 2004, 287:H1792–H1800
48. Hangai-Hoger N, Tsai AG, Friesenecker B, Cabrales P, Intaglietta M: Microvascular oxygen delivery and consumption following treatment with verapamil. Am J Physiol 2005, 288:H295–H300
49. Ball HJ, MacDougall HG, McGregor IS, Hunt NH: Cyclooxygenase-2 in the pathogenesis of murine cerebral malaria. J Infect Dis 2004, 189:751–758
50. Deininger MH, Kremsner PG, Meyermann R, Schluesener HJ: Focal accumulation of cyclooxygenase-1 (COX-1) and COX-2 expressing cells in cerebral malaria. J Neuroimmunol 2000, 106:198–205
51. Xiao L, Patterson PS, Yang C, Lal AA: Role of eicosanoids in the pathogenesis of murine cerebral malaria. Am J Trop Med Hyg 1999, 60:668–673
52. Grau GE, Fajardo LF, Piguet PF, Allet B, Lambert PH, Vassalli P: Tumor necrosis factor (cachectin) as an essential mediator in murine cerebral malaria. Science 1987, 237:1210–1212
53. Grau GE, Piguet PF, Vassalli P, Lambert PH: Tumor-necrosis factor and other cytokines in cerebral malaria: experimental and clinical data. Immunol Rev 1989, 112:49–70
54. Grau GE, Taylor TE, Molyneux ME, Wirima JJ, Vassalli P, Hommel M, Lambert PH: Tumor necrosis factor and disease severity in children with falciparum malaria. N Engl J Med 1989, 320:1586–1591
55. Stoelcker B, Hehlgans T, Weigl K, Bluethmann H, Grau GE, Mannel DN: Requirement for tumor necrosis factor receptor 2 expression on vascular cells to induce experimental cerebral malaria. Infect Immun 2002, 70:5857–5859.